Chapter 13
A Novel Aggregation Technique Using Mechanical Torque Compensating Factor for DFIG Wind Farms

M. A. Chowdhury

Abstract A novel aggregated model for wind farms consisting of wind turbines equipped with doubly fed induction generators (DFIG) is proposed in this paper. In the proposed model, a mechanical torque compensating factor (MTCF) is integrated into a full aggregated wind farm model to deal with the nonlinearity of wind turbines in the partial load region and to make it behave as closely as possible to a complete model of the wind farm. The MTCF is initially constructed to approximate a Gaussian function by a fuzzy logic method and optimized on a trial and error basis to achieve less than 10% discrepancy between the proposed aggregated model and the complete model. Then, a large scale offshore wind farm comprising 72 DFIG wind turbines is used to verify the effectiveness of the proposed aggregated model. The simulation results show that the proposed model is able to approximate collective dynamic responses at the point of common coupling with significant reduction in the simulation computation time.

Keywords Doubly fed induction generator · Wind farm · Aggregated model · Mechanical torque compensating factor · Fuzzy logic

13.1 Introduction

Wind power has been the fastest growing energy source since the last decade due to its inherent attribute of the reproducible, resourceful and pollution-free characteristics. Wind power capacity reached 215 GW (3 % of global electricity consumption) worldwide with a growth rate of 22.9 % in 2010. With this growth rate, wind power capacity will be doubled every 3 years. Based on this accelerated

M. A. Chowdhury (✉)
Faculty of Engineering and Industrial Sciences, Swinbune University of Technology,
Internal Mail H38, PO Box 218, Hawthorn, VIC 3122, Australia
e-mail: achowdhury@swin.edu.au

J. Hossain and A. Mahmud (eds.), *Renewable Energy Integration*,
Green Energy and Technology, DOI: 10.1007/978-981-4585-27-9_13,

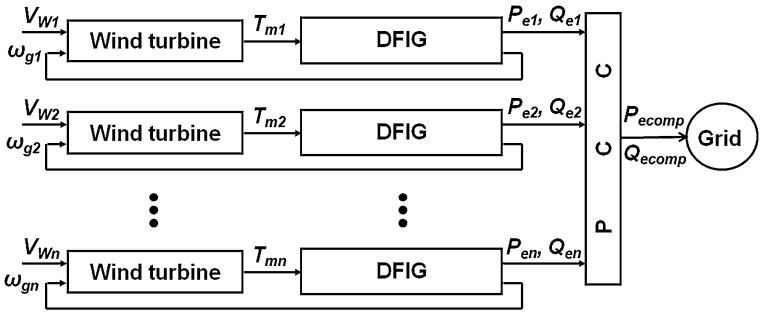

Fig. 13.1 Block diagram of a complete DFIG wind farm model

development and further improved policies, 12 % of global electricity demand (1900 GW) is predicted to be provided by wind energy systems by the year 2020 [1].

Wind farms of 50 MW ratings or more are integrated into high voltage transmission networks [2]. With the increasing amount of wind power penetration in power systems, wind farms begin to influence power systems. This justifies the need for adequate models for wind farms in order to represent overall power system dynamic behavior of grid-connected wind farms during both normal operations and grid disturbances. A wind farm may consist of tens to hundreds of wind turbines. This leads to model complexity and computation burden [3, 4]. Figure 13.1 shows a complete wind farm model with n number of wind turbines equipped with doubly-fed induction generator (DFIG).

To simplify the complete wind farm model, an aggregated wind farm model is required to reduce the size of the power system model, the data requirement and the simulation computation time [5–7], where this aggregated model can (1) represent the behavior (active and reactive power exchanged with the power system at the point of common coupling (PCC)) of the wind farm during normal operation, characterized by small deviations of the grid quantities from the nominal values and the occurrence of wind speed changes and (2) represent the behavior of the wind farm during grid disturbances, such as voltage drops and frequency deviations.

Two types of wind farm aggregation techniques have been proposed: the full aggregated and the semi aggregated techniques. Figure 13.2 shows the full aggregated and semi aggregated wind farm models. The full aggregated model consists of one equivalent wind turbine and one equivalent generator for a wind farm with one operating point at an average wind speed for all the wind turbines in the wind farm [7–12]. The semi aggregated model consists of all the wind turbines in the wind farm and one equivalent generator [13, 14].

For a wind farm consisting of DFIG wind turbines, the ability of the full or semi aggregated model to approximate the complete model depends on the operating region of the DFIG wind turbines. The operating regions of the DFIG wind turbine adopted in this work is shown in Fig. 13.3, which can be segmented into two parts: a partial load region, where the wind speed ranges between 4.5 and 14.5 m/s and a

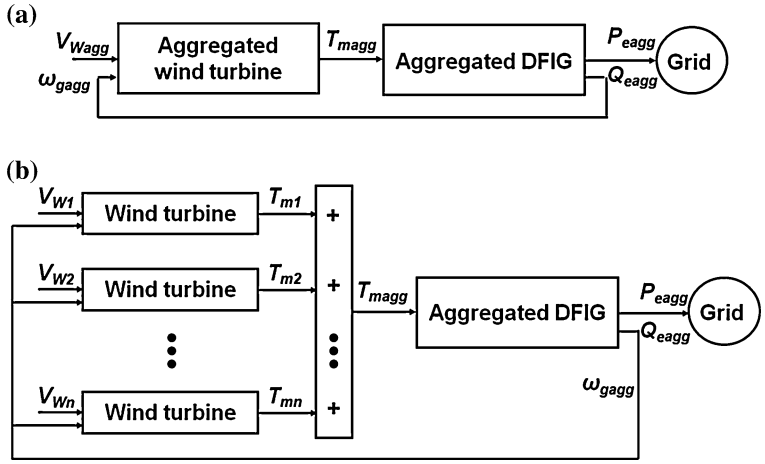

Fig. 13.2 Block diagram of **a** full aggregated and **b** semi aggregated DFIG wind farm models

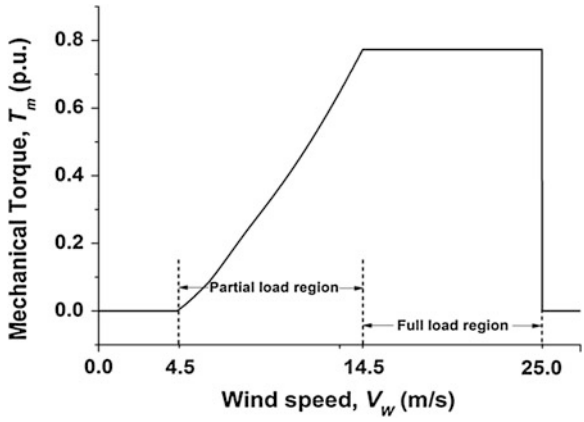

Fig. 13.3 Operating regions of the DFIG wind turbine at the turbine rotor speed of 1 p.u

full load region, where the wind speed ranges between 14.5 and 25 m/s).The DFIG wind turbine is stopped when wind speed is less than 4.5 m/s or greater than 25 m/s.

The full or semi aggregated model can represent the complete model when DFIG wind turbines in the wind farm operate in the full load region regardless of the differences in the operating points of the wind turbines in the wind farm. This is due to the fact that all generators produce the same current at its maximum rating in this region.

But, the full aggregated model cannot provide an accurate approximation of a complete model when DFIG wind turbines in the wind farm operate in the partial load region. This is due to the fact that the full aggregated technique does not consider the operating points of all corresponding wind turbines in the wind farm and a nonlinear relationship between wind speed (V_W) and mechanical torque (T_m) as shown in Fig. 13.3.

The semi aggregated model, on the other hand, improves the approximation of a complete model in the partial load region by considering the operating points of all corresponding wind turbines in the wind farm. The use of an average generator rotor speed (ω_g) for all of the wind turbines still contributes to discrepancies in the magnitude of mechanical torque and consequently electromagnetic torque.

This chapter thus proposes a new aggregation technique with the incorporation of a mechanical torque compensation factor (MTCF) into the full aggregated wind farm model to deal with the nonlinearity of wind turbines in the partial load region and to make it behave as closely as possible to a complete model of the wind farm.

13.2 DFIG Wind Turbine Model

The DFIG wind turbine is modelled in terms of behavior equations of each of the subsystems, mainly the turbine, the drive train, the induction generator and the control system (Fig. 13.4).

The aerodynamics of the wind turbine is characterized by *Cp*-λ-β curve. *Cp* is the power coefficient, which corresponds to maximum mechanical power extraction from wind for its maximum value, and is a function of the tip-speed ratio (λ) and the pitch angle (β), which is given by [15]

$$C_p(\lambda, \beta) = 0.22\left(\frac{116}{\lambda_i} - 0.4\beta - 5\right)e^{\frac{-12.5}{\lambda_i}} \tag{13.1}$$

where

$$\frac{1}{\lambda_i} = \frac{1}{\lambda + 0.08\beta} - \frac{0.035}{\beta^3 + 1} \tag{13.2}$$

For a given *Cp,* the mechanical torque (T_m) produced by the wind turbine is given by [16]

$$T_m = \frac{\rho A C_p V_W^3}{2\omega_t} \tag{13.3}$$

where ρ is the air density, A is the sweep area of the blades, V_W is the wind speed and ω_t is the turbine rotor speed.

For modeling drive train, the rotor is treated as two lumped masses, i.e., turbine mass and generator mass are connected together by shaft with a certain damping and stiffness coefficient values [17].

After simplifications by neglecting the turbine and generator self-damping, shaft stiffness and torsional oscillations, the mathematical equation can be expressed

$$2H\frac{\mathrm{d}\omega_g}{\mathrm{d}t} = T_m - T_e \tag{13.4}$$

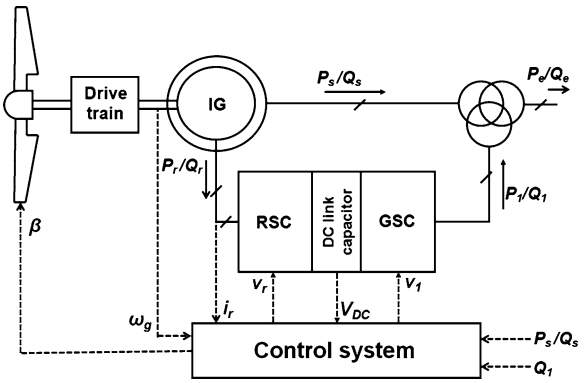

Fig. 13.4 Configuration of a DFIG wind turbine

where H is the inertia constant, ω_g is the generator rotor speed and T_e is the electromagnetic torque.

For modeling induction generator, a synchronously rotating d-q reference frame is chosen, which is rotating with the same speed as the stator voltage. Stator and rotor voltages in this reference frame are given by

$$v_{ds} = -R_s i_{ds} - \omega_s \phi_{qs} + \frac{d\phi_{ds}}{dt} \tag{13.5}$$

$$v_{qs} = -R_s i_{qs} + \omega_s \phi_{ds} + \frac{d\phi_{qs}}{dt} \tag{13.6}$$

$$v_{dr} = -R_r i_{dr} - s\omega_s \phi_{qr} + \frac{d\phi_{dr}}{dt} \tag{13.7}$$

$$v_{qr} = -R_r i_{qr} + s\omega_s \phi_{dr} + \frac{d\phi_{qr}}{dt} \tag{13.8}$$

where v is the voltage, i is the current, R is the resistance, ω_s is the synchronous speed, ϕ is the flux and s is the slip. Suffix s, r, d and q denote stator, rotor, d-axis component and q-axis component, respectively.

The electromagnetic torque (T_e) is expressed in [18] as

$$T_e = \phi_{ds} i_{qs} - \phi_{qs} i_{ds} \tag{13.9}$$

where p is the number of poles.

The output active and reactive powers (P_e and Q_e) are then calculated as

$$P_e = v_{ds} i_{ds} + v_{qs} i_{qs} + v_{dr} i_{dr} + v_{qr} i_{qr} \tag{13.10}$$

$$Q_e = v_{qs} i_{ds} - v_{ds} i_{qs} + v_{qr} i_{dr} - v_{dr} i_{qr} \tag{13.11}$$

Table 13.1 DFIG wind turbine parameters

Parameter	Symbol	Value	Unit
Nominal mechanical output power	P_{mec}	1.5	MW
Nominal electrical power	P_{elec}	1.5/0.9	MW
Nominal voltage (L–L)	V_{nom}	575	Volt
Stator resistance	R_s	0.00706	p.u.
Stator leakage inductance	L_r	0.171	p.u.
Rotor resistance	R_r	0.0058	p.u.
Rotor leakage inductance	L_r	0.156	p.u.
Magnetizing inductance	L_m	2.9	p.u.
Base frequency	f	60	Hz
Inertia constant	H	1	s
Friction factor	F	0.01	p.u.
Pair of poles	p	3	–

The control system comprises of two external power electronic converter controllers and a pitch angle controller. These controllers are modelled by the conventional PI controllers [19]. The converter controllers generate the voltage command signal v_r and v_1 for the rotor side converter (RSC) and grid side converter (GSC), respectively in order to control the DC voltage and the reactive power or the voltage at the grid terminals. The pitch angle controller generates pitch angle command signal (β) for temporary reduction of mechanical power when the DFIG wind turbine operates in the full load region. Their detail explanation can be found in [20]. The parameters of the DFIG wind turbine used in this work are shown in Table 13.1 [21].

13.3 Formation of a Complete DFIG Wind Farm Model

The model of a wind farm with all of its electrical networks is presented in this section, which is a modified version of a 120 MVA offshore wind farm model implemented by 'NESA Transmission Planning' of Denmark for power stability investigations [8] as shown in Fig. 13.5. The wind farm model comprises of 72 DFIG wind turbines with the parameters specified in Table 13.1. Each WTG is connected to the cable sections through 0.67/30 kV transformer (LV/MV) and a line impedance of $0.08 + j0.02$ p.u. The wind farm is connected to the power grid through a 30/132 kV tertiary transformer (MV/HV) and then through a high voltage (132 kV) transmission network (HVTN) with the impedance value of $1.6 + j3.5$ p.u.

The internal and external electrical networks including electric lines, transformers and cables are represented by constant impedances [13]. Short circuit capacity viewed from the PCC into the HVTN is around 1500 MVA. The power grid is modeled by an infinite bus with the MVA-rating of 1000 MVA.

A pair of indices identifies the WTG within the wind farm, where the first index (from 1 to 6) denotes the number of the group (the 30 kV sea cable) and the second

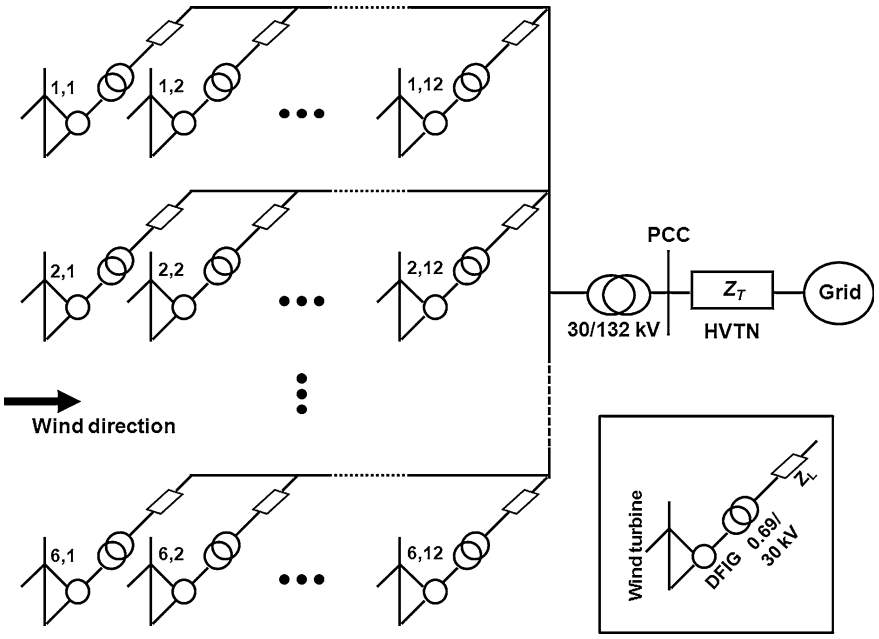

Fig. 13.5 A 120 MVA offshore DFIG wind farm model

Table 13.2 DFIG wind farm parameters

Parameter	Symbol	Value	Unit
Internal electrical network			
Base power	S_{WTG}	1.5/0.9	MVA
Base voltage	V_{WTG}	575	V
LV/MV transformer	–	0.69/30	kV
	S_T	2	MVA
	ε_{cc}	6	%
Line impedance	Z_L	0.08 + j0.02	p.u.
External electrical network			
MV/HV transformer	–	30/132	kV
	S_T	150	MVA
	ε_{cc}	8	%
HVTN impedance	Z_T	1.6 + j3.5	p.u.
Short circuit capacity of the PCC	S_{PCC}	1500	MVA
X/R ratio of PCC	$(X/R)_{PCC}$	20	p.u.
Short circuit capacity of the grid	S_G	1000	MVA

index (from 1 to 12) denotes the number of the WTG within the group. The parameters of the DFIG wind farm used in the simulation are shown in Table 13.2 [8, 13].

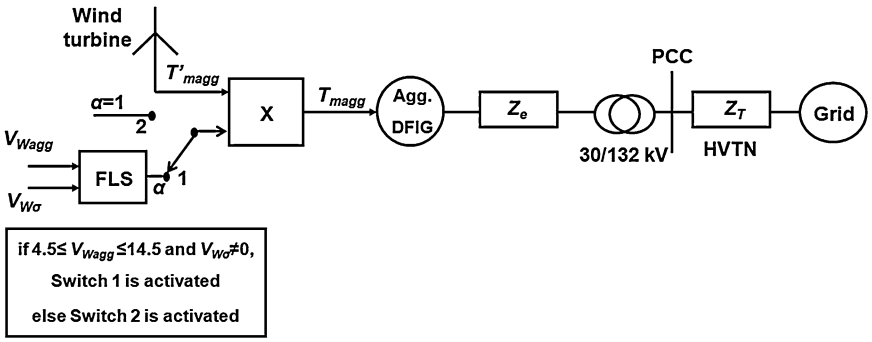

Fig. 13.6 Block diagram of the proposed aggregated DFIG wind farm model

13.4 Proposed Aggregated DFIG Wind Farm Model

Figure 13.6 shows the proposed aggregated DFIG wind farm model that consists of a mechanical torque compensating factor (MTCF) incorporated into a traditional full aggregated model. The MTCF (α) is a multiplication factor to the mechanical torque (T'_{magg}) of the full aggregated model that minimizes this inaccuracy in approximation. The mechanical torque (T_{magg}) of the proposed aggregated DFIG wind farm model is thus calculated by

$$T_{magg} = T'_{magg} * \alpha \tag{13.12}$$

The proposed model also involves the calculation of an equivalent internal network and the simplification of the power coefficient (C_p) function.

13.4.1 Full Aggregated DFIG Wind Farm Model

The full aggregated DFIG wind farm model converts all DFIG wind turbines in the wind farm into one equivalent unit with the same per unit value of mechanical and electrical parameters in the voltage, flux linkage and motion equations [13], which is driven by an average wind speed (V_{Wagg}) [14]

$$V_{Wagg} = \frac{1}{n}\sum_{i=1}^{n} V_{Wi} \tag{13.13}$$

where n is the number of WTGs in the wind farm and suffix agg denotes the aggregated wind farm model.

This gives the mechanical torque as

$$T'_{magg} = \frac{\rho A C_p V_{Wagg}^3}{2\omega_{tagg}} \tag{13.14}$$

where ω_{tagg} is the average turbine rotor speed calculated from V_{Wagg}.

13.4.2 Basis of MTCF Calculation

As stated earlier, the full aggregated model can provide an approximation of the complete model when DFIG wind turbines operate in the full load region. Thus, in this region the MTCF takes a value equal to 1.

When the wind turbines operate at different wind speeds and thus different operating points, the adoption of an average operating point for the DFIG wind turbines causes the discrepancies between the complete and full aggregated models. Figure 13.7 shows that the torque of the full aggregated model is generally lower than that of the complete model in the partial load region. Thus, in this region the MTCF takes a value more than 1.

It means that the MTCF increases from the value 1 as V_{Wagg} increases from 4.5 m/s or V_{Wagg} decreases from 14.5 m/s, which implies that the MTCF may take its maximum value between 4.5 and 14.5 m/s. On the other hand, the MTCF maintains a proportional relation with the wind speed deviation ($V_{W\sigma}$) and it takes a value equal to 1 when the operating points of the DFIG wind turbines in the wind farm are identical (i.e., $V_{W\sigma} = 0$). Thus, the MTCF is a function of V_{Wagg} and $V_{W\sigma}$ and may be 'approximated' by an ideal Gaussian function (see Fig. 13.8) in the partial load region:

$$\alpha = 1 + le^{\frac{-(V_{Wagg} - V_{W\mu})^2}{2\sigma^2}} V_{W\sigma} \tag{13.15}$$

According to Eq. 13.15, the maximum value of α is $(1 + l)$ when the wind speed is equal to $V_{W\mu}$ (in this work, $V_{W\mu} = 9.5$ m/s) and σ is the standard deviation from $V_{W\mu}$.

From empirical rule of the central limit theorem, it is known that 99.993 % of data lie within four standard deviation from their mean value [22]. It gives the value of σ and l.

$$4\sigma = 5 \tag{13.16}$$

$$l = \frac{1}{\sigma\sqrt{2\pi}} = 0.32 \tag{13.17}$$

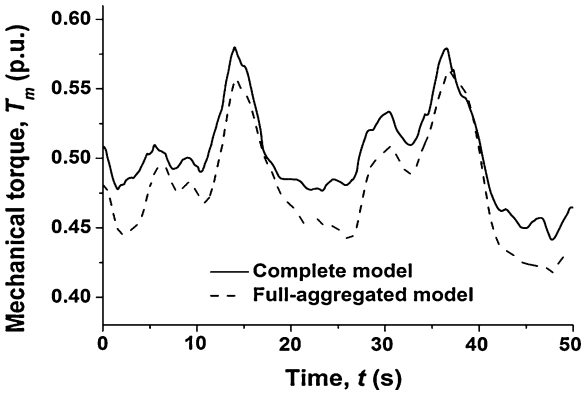

Fig. 13.7 Torque curves of the complete and full aggregated model in the partial load region

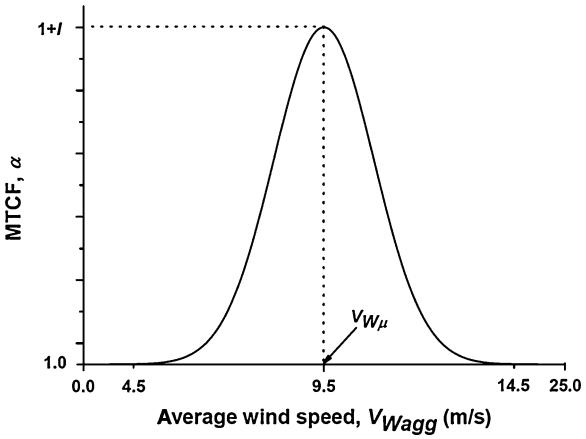

Fig. 13.8 Gaussian distribution of MTCF (α) with respect to average wind speed (V_{Wagg})

13.4.3 MTCF Calculation by Fuzzy Logic System

Due to the complex nonlinear relationship and ambiguous dynamics of the wind energy generation system, it is difficult to find the mathematical model for the input–output relationship for the calculation of the MTCF. However, based on the expert (operator's) knowledge, a human operator can express the input–output relationship of a MTCF by using linguistic rules without knowing the exact mathematical relationship and this expert knowledge described by linguistic rules can be used to design the fuzzy logic system (FLS), which makes the FLS a very good candidate to compute the MTCF. Thus, the FLS is adopted to calculate the MTCF in this work.

The FLS is initially constructed by assigning overlapped triangular membership functions for the fuzzy sets and setting fuzzy rules based on the ideal Gaussian function. Triangular membership functions are easy to implement, quicker to process and give more sensitivity, especially as variables approach to zero.

The design is optimized by making possible changes in membership functions for the fuzzy sets and fuzzy rules on trial and error basis to achieve less than 10 % discrepancy between the proposed aggregated model and the complete model.

The FLS takes two inputs: average wind speed (V_{wagg}) and wind speed deviation ($V_{W\sigma}$). In the design of the FLS, V_{wagg} ranges between 4.5 and 14.5 m/s. $V_{W\sigma}$ ranges between 0 and its maximum possible value. The value of $V_{W\sigma}$ is the maximum when wind speeds received by the wind turbines are equally spaced within the specified range of V_{Wagg}. For 72 DFIG wind turbines, the maximum value of $V_{W\sigma}$ is found by the following calculation:

$$V_{W\sigma\max} = \sqrt{\frac{1}{72}\sum_{i=1}^{72}\left(\frac{14.5-4.5}{72-1}i - 9.5\right)^2} = 5.25 \tag{13.18}$$

Then, according to Eq. 13.15, the MTCF (α) is 2.7 when $V_{Wagg} = V_{W\mu}$ and $V_{W\sigma} = 5.25$ (takes its maximum value), thus the range of the MTCF should be between 1 and 2.7.

Figure 13.9 shows that triangular membership functions are assigned to each input or output variable. It has been selected 7 membership functions for V_{Wagg}, 7 for $V_{W\sigma}$ and 8 for output α. Overall 49 (i.e., 7 × 7) rules are built by crossing the fuzzy sets, as shown in Table 13.3.

The *i*th fuzzy rule is expressed as [23]

Rule *i*: if V_{Wagg} is A_a and $V_{W\sigma}$ is B_b,

$$\text{then } \alpha(n) \text{ is } C_c. \tag{13.19}$$

$a = 1, 2, \ldots, 7$; $b = 1, 2, \ldots, 7$; $c = 1, 2, \ldots, 49$

where A_a and B_b denote the antecedents and C_c is the consequent part.

The FLS gives the values of the MTCF (α) by applying the center of gravity method [23]

$$\alpha(n) = \sum_{i=1}^{49} \omega_i C_c \Big/ \sum_{i=1}^{49} \omega_i \tag{13.20}$$

where ω_i denotes the grade for the antecedent, which is the product of grade for the antecedents of each rule.

13.4.4 Equivalent Internal Electrical Network

The aggregated wind farm must operate at an equivalent internal electrical network. Thus, the internal electrical network of each individual DFIG wind turbine in the complete model is required to be replaced by equivalent impedance in the proposed aggregated wind farm model. The short circuit impedance of the aggregated wind

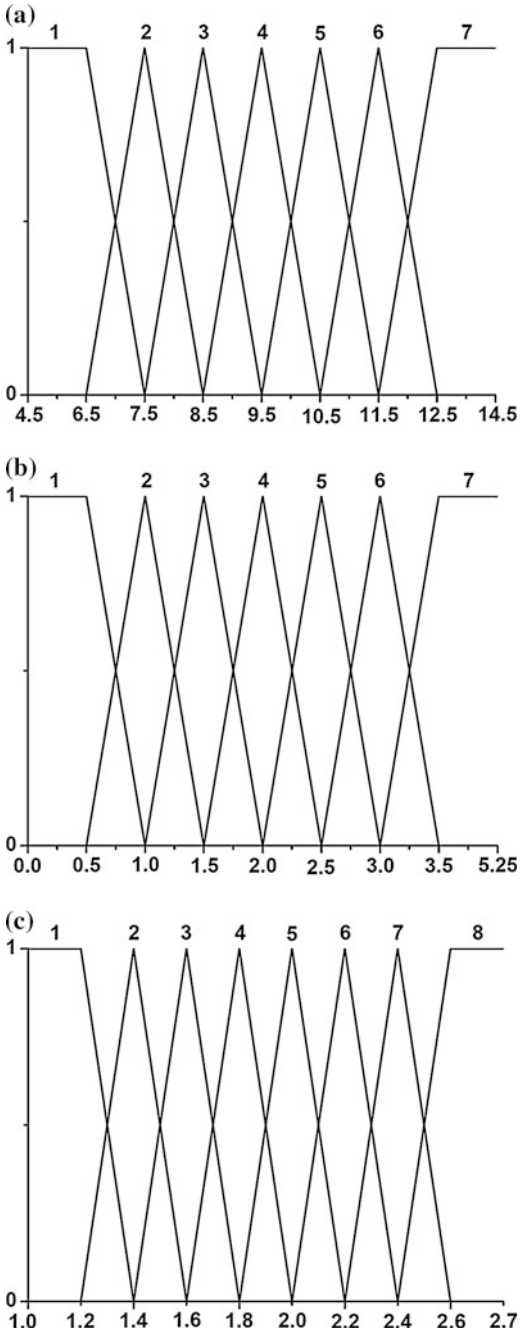

Fig. 13.9 Membership functions: **a** V_{Wagg}, **b** $V_{W\sigma}$ and **c** α

Table 13.3 Rules of the FLS

α		$V_{W\sigma}$						
		1	2	3	4	5	6	7
V_{Wagg}	1	1	1	1	2	3	3	4
	2	1	1	2	3	3	4	5
	3	1	2	3	3	5	6	7
	4	2	3	4	5	6	7	8
	5	1	2	3	4	5	6	7
	6	1	1	2	3	4	5	6
	7	1	1	2	3	3	4	5

farm must be equal to that of the complete wind farm, which gives the calculation of the equivalent impedance (Z_e) of the aggregated wind farm [13]

$$Z_e = Z_{awt} - \frac{Z_{wt}}{n} \tag{13.21}$$

where Z_{awt} is the equivalent impedance of the internal electrical network of each individual DFIG wind turbine in the complete model, Z_{wt} is the impedance of DFIG wind turbine.

13.4.5 Model Simplification

The detailed representation of wind farms with DFIG wind turbines is quite complex. However, it can be simplified assuming that the power coefficient (C_p) is always equal to the maximum value because the control mechanism of the DFIG wind turbine maintains its power-speed characteristics such that C_p is always tracking its maximum value (in this work, $C_{pmax} = 0.48$) [24]. Due to the adoption of the maximum power coefficient, the complicated $C_p(\lambda, \beta)$ characteristics from the model (Eq. 13.1) is replaced by the transfer characteristics by a first order approximation (see Fig. 13.10).

13.4.6 Simulation Results

Both the proposed aggregated model and the full aggregated model are simulated to obtain the dynamic responses at the PCC under the following two conditions: (1) normal operation and (2) grid disturbance. The variables considered for the comparison are the active (P_e) and reactive power (Q_e) exchange between the wind farm and power system. The reactive power is taken into the calculation of the proposed aggregated model because the reactive power does not solely depend on active power generation in the DFIG wind turbine, where the reactive power and

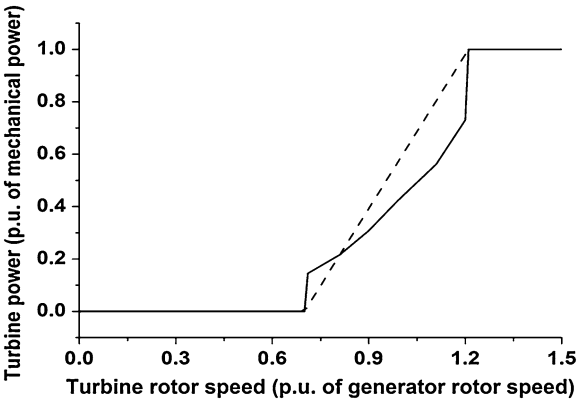

Fig. 13.10 First order approximation (*dashed line*) of transfer characteristic (*solid line*) of the DFIG wind turbine

active power are independently regulated by the converter controllers in the exchange of reactive power with the grid. In addition, the operation in the dynamic speed range could demand lower reactive power output due to increased active power output at higher and gusty wind conditions [25].

Figure 13.11 shows the speed of the wind received by the first DFIG wind turbine in each group. The time delay and wake effect are accounted for approximating wind speed for the following DFIG wind turbines in each corresponding group.

Any changes in wind speed upstream have effects on the wind speed downstream after a certain time delay due to the wind speed transport. The delay is a function of distance and wind speed. The transport time delay of wind speed (t_{delay}) passing between two successive columns can be roughly estimated using [26]

$$t_{delay} = \frac{d}{\overline{V_W}} \tag{13.22}$$

where d is the distance between the two successive turbine columns and $\overline{V_W}$is the average wind speed passing the first DFIG wind turbine.

Power extraction on wind flow passing the turbine creates a wind speed deficit in the area behind the turbine. This phenomenon is known as 'wake effect'. As a consequence, the turbines that are located downstream obtain lower wind speed than those that are located upstream. The deficit in wind speed due to the wake effect depends on several factors, such as the distance behind turbine, turbine efficiency and turbine rotor size. Wind speed in the wake at a distance x behind the turbine rotor can be calculated as [27]

$$V_W(x) = V_o\left[1 - \left(\frac{R}{k_w x + R}\right)^2\left(1 - \sqrt{1 - C_T}\right)\right] \tag{13.23}$$

where V_o is the incoming free-stream wind speed, C_T is the turbine thrust coefficient whose value is adopted from [28] and k_w is the wake decay constant.

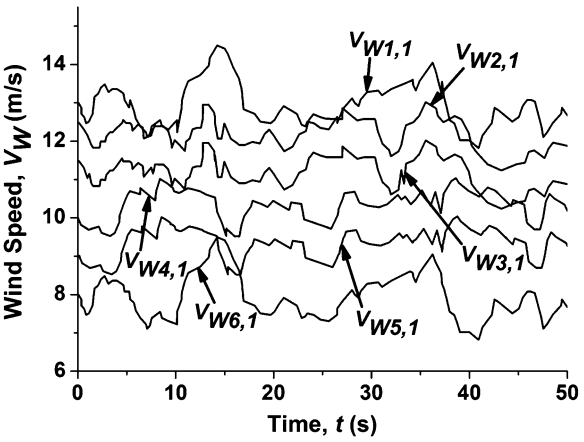

Fig. 13.11 Wind speed received by the first DFIG wind turbine in each group

13.4.7 Normal Operation

The collective responses of the complete, the full aggregated and the proposed aggregated wind farm models at the PCC during normal operation are shown in Fig. 13.12.

The proposed aggregated model has a higher correspondence in approximating active power (see Fig. 13.12a). Comparing with the complete model, it has the maximum and average discrepancy of 2.94 and 2.35 %, respectively, while the full aggregated model has the maximum and average discrepancy of 8.23 and 6.58 %, respectively. The multiplication factor MTCF, dynamically produced by a well-tuned FLS, manipulates the mechanical torque to compensate the existing non-linearities in the wind farm in order to have a better approximation in the proposed aggregated model. The proposed aggregated model cannot respond to the high frequency fluctuations of wind speed as compared to the complete model, as can be seen during periods of time between 23 and 26.5 s and between 37.5 and 50 s.

The proposed aggregated model has a higher correspondence in approximating reactive power as well (see Fig. 13.12b). Comparing with the complete model, it has the maximum and average discrepancy of 5.45 and 4.36 %, respectively, while the full aggregated model has the maximum and average discrepancy of 9 and 8.14 %, respectively. The reactive power for DFIG wind turbine depends on the active power and the generation voltage. These variables differ in each DFIG wind turbine when the incoming winds are different. Therefore, it leads to different converter controller action for each DFIG wind turbine. This is not accounted for in the aggregated model resulting in lesser accuracy in the approximation of reactive power at the PCC. The manipulation of mechanical torque in the proposed aggregated model enables it to provide a better performance. However, poor approximation of reactive power is observed during the periods between 13 and 18 s and between 34.5 and 38 s.

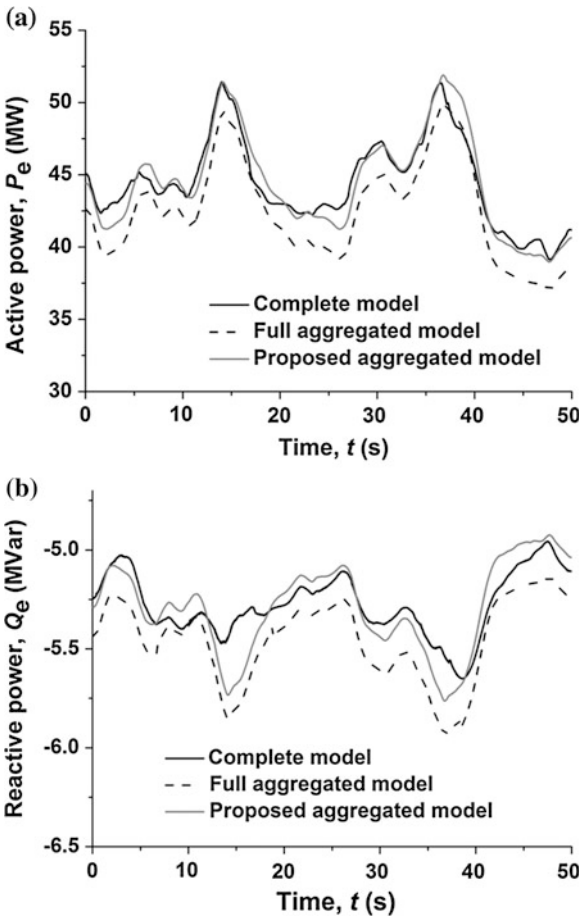

Fig. 13.12 Evaluation of the proposed aggregated wind farm model during normal operation at the PCC: **a** Active power and **b** Reactive power

13.4.8 Grid Disturbance

A voltage sag of 50 % lasting for 0.1 s is originated at the PCC at $t = 1$ s to evaluate the proposed aggregated wind farm model during grid disturbances, the collective responses of the complete, the full aggregated and the proposed aggregated wind farm models at the PCC are shown in Fig. 13.13.

Figure 13.13 shows that the active power produced by the wind farm reduces and it goes to negative values for a short time (i.e. the grid supplies active power to the DFIG to keep it spinning) during grid disturbances. On the other hand, the reactive power which is normally negative (which means the wind farm takes reactive power from the grid) changes sign and increases during the disturbance. This means the wind farm supplies reactive power to the grid during the disturbance caused by the voltage sag.

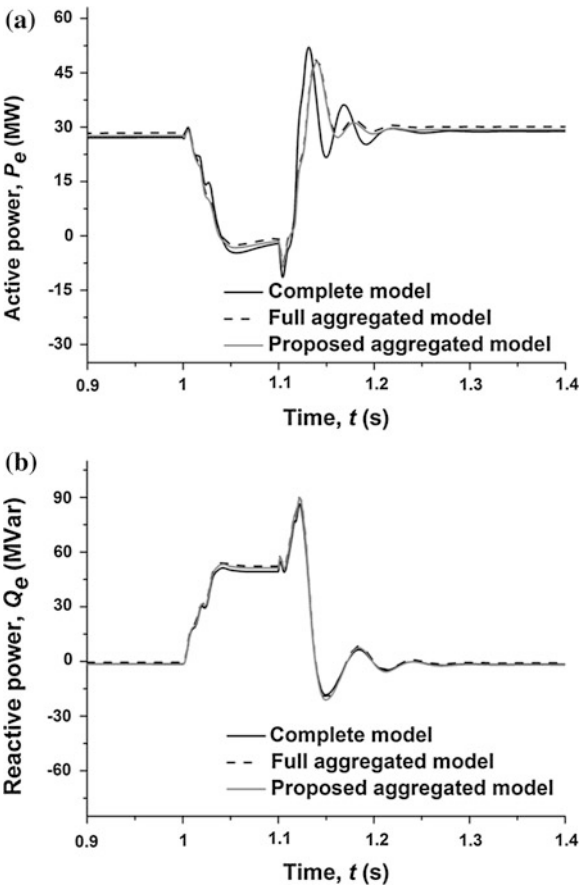

Fig. 13.13 Evaluation of the proposed aggregated wind farm model during grid disturbance at the PCC: **a** Active power and **b** Reactive power

It also shows a high correspondence among the collective responses at the PCC of the complete, the full aggregated and the proposed aggregated wind farm models with negligible discrepancies on the active and reactive power. However, the active power (P_e) slightly mismatches in both aggregated models right after clearing the fault when different parameters start retaining their normal values. This high level of correspondence is partly due to the fact that the grid disturbances are much faster than the wind speed variations [13] and, therefore, the discrepancies during normal operations are unimportant during grid disturbances.

13.5 Evaluation of the Proposed Aggregated Technique

In previous section, the good agreement of the collective responses at the PCC between the proposed aggregated model and the complete model verifies the stability of the aggregated model. In the following, the proposed aggregated

Table 13.4 Accuracy in approximating the collective responses at the PCC

Operation type	Full aggregated model		Proposed aggregated model	
Normal operation	n_{Pe} (%)	91.3	n_{Pe} (%)	100
	n_{Qe} (%)	87.5	n_{Qe} (%)	100
Grid disturbance	n_{Pe} (%)	95	n_{Pe} (%)	95
	n_{Qe} (%)	100	n_{Qe} (%)	100

technique is evaluated in terms of the accuracy in the approximation of the collective responses at the PCC, such as active power (P_e) and reactive power (Q_e) and simulation computation time.

13.5.1 Accuracy in Approximation

The discrepancy between any instantaneous output power of the proposed aggregated model and that of the complete model can be calculated by the following equation [29]

$$\Delta x = \left| \frac{x_{comp} - x_{agg}}{x_{comp}} \right| \tag{13.24}$$

where x can be either active power (P_e) or reactive power (Q_e). Suffix *comp* denotes the complete wind farm model.

The results of the accuracy in approximating the collective responses are shown in Table 13.4, where n_{Pe} and n_{Qe} are the number of instantaneous values of active and reactive power, respectively. It shows that less than 10 % discrepancy has been achieved between the proposed aggregated model and the complete model. It can be seen as well that in normal operation the proposed aggregated model approximates active power (P_e) and reactive power (Q_e) more accurately than the full aggregated model by 8.7 and 12.5 %, respectively. However, in grid disturbance both models show the same level of accuracy.

13.5.2 Simulation Computation Time

The comparison of computation time for the complete and both aggregated wind farm models are made and the results are shown in Table 13.5. The simulations are carried out on a personal computer with the following specifications: Intel (R) Pentium (R) Dual CPU E2200, 2.20 GHz, 1.96 GB of RAM.

It can be seen that the proposed aggregated wind farm model has higher simulation computation time than the full aggregated wind farm model by 2.38 and 3 % during normal operation and grid disturbance, respectively. A slight increase

Table 13.5 Comparison of simulation computation time

Operation type	Simulation computation time (s)			Reduction in simulation time (%)	
	Complete model	Full aggregated model	Proposed aggregated model	Full aggregated model	Proposed aggregated model
Normal operation	1476	110	142	92.5	90.3
Grid disturbance	2283	235	298	89.7	87

in the computation time is caused by the additional computing block with the FLS to generate the MTCF. However, it has significantly reduced the simulation computation time by 90.3 and 87 %, respectively, comparing with the complete model during normal operation and grid disturbance.

13.6 Conclusions

This chapter describes the development of a novel aggregated technique with the incorporation of a mechanical torque compensation factor (MTCF) into the full aggregated wind farm model to obtain dynamic responses of a wind farm at the point of common coupling. The aim is to simulate the dynamic responses of the wind farm with an acceptable level of accuracy while reducing the simulation time considerably by using the aggregation technique. The MTCF is a multiplication factor to the mechanical torque of the full aggregated wind farm model that is initially constructed to approximate a Gaussian function by a fuzzy logic method and optimized on a trial and error basis to achieve less than 10 % discrepancy between the proposed aggregated model and the complete model. The proposed aggregated model is then applied to a bigger 120 MVA offshore wind farm comprising of 72 DFIG wind turbines. Simulation results show that the proposed aggregated wind farm model has the average discrepancy in approximating active power (P_e) and reactive power (Q_e) of 2.35 and 4.36 %, respectively, during normal operation as compared to the complete model. But it has 8.7 and 12.5 % more approximation capability of P_e and Q_e, respectively, than the full aggregated model. However, the proposed aggregated model can mimic P_e and Q_e with negligible discrepancy during grid disturbance. Computational time of the proposed aggregated model is slightly higher than that of the full aggregated model but much faster than the complete model by 90.3 % during normal operation and 87 % during grid disturbance.

References

1. Executive Summary (2011) World wind energy report 2011. http://www.wwindea.org/home/index.php. Accessed 15 Nov 2011
2. [2] Li L, Jing Z, Yihan Y (2009) Comparison of pitch angle control models of wind farm for power system analysis. In: IEEE power and energy society general meeting, Calgary, pp 1-7 July 2009
3. Rodriguez-Amenedo JL, Arnalte S, Burgos JC (2002) Automatic generation control of a wind farm with variable speed wind turbines. IEEE Trans Energy Convers 17:279–284
4. Tapia A, Tapia G, Ostolaza JX, Saenz JR, Criado R, Berasategui JL (2001) Reactive power control of a wind farm made up with doubly fed induction generators. In: IEEE Power Tech Proceedings, Porto, p 6, September 2001
5. Feijóo A, Cidrás J, Carrillo C (2000) A third order model for the doubly-fed induction machine. Elect Power Syst Res 56:121–127
6. Ekanayake JB, Holdsworth L, XueGuang W, Jenkins N (2003) Dynamic modeling of doubly fed induction generator wind turbines. IEEE Trans Power Syst 18:803–809
7. Nunes MVA, Lopes JAP, Zurn HH, Bezerra UH, Almeida RG (2004) Influence of the variable-speed wind generators in transient stability margin of the conventional generators integrated in electrical grids. IEEE Trans Energy Convers 19:692–701
8. Akhmatov V, Knudsen H (2002) An aggregate model of a grid-connected, large-scale, offshore wind farm for power stability investigations—importance of windmill mechanical system. Int J Electr Power Energy Syst 24:709–717
9. Usaola J, Ledesma P, Rodriguez JM, Fernandez JL, Beato D, Iturbe R et al. (2003) Transient stability studies in grids with great wind power penetration. Modelling issues and operation requirements. In: IEEE power engineering society general meeting, Toronto, p 1541, July 2003
10. Ledesma P, Usaola J, Rodríguez JL (2003) Transient stability of a fixed speed wind farm. Renewable Energy 28:1341–1355
11. Slootweg JG, Kling WL (2003) Aggregated modelling of wind parks in power system dynamics simulations. In: IEEE power tech conference proceedings, Bologna, p 6, June 2003
12. Fernández LM, García CA, Saenz JR, Jurado F (2009) Equivalent models of wind farms by using aggregated wind turbines and equivalent winds. Energy Convers Manage 50:691–704
13. Fernández LM, Jurado F, Saenz JR (2008) Aggregated dynamic model for wind farms with doubly fed induction generator wind turbines. Renewable Energy 33:129–140
14. Poller M, Achilles S (2003) Aggregated wind park models for analyzing power system dynamics. In: Proceedings of the international workshop on large scale integration of wind power and transmission networks for offshore wind farms, Billund, Oct 2003
15. Perdana A, Carlson O, Persson J (2004) Dynamic response of grid-connected wind turbine with doubly fed induction generator during disturbances. In: Proceedings of the IEEE Nordic workshop on power and industrial electronics, Trondheim, June 2004
16. Sedaghat A, Mirhosseini M (2012) Aerodynamic design of a 300 kW horizontal axis wind turbine for province of Semnan. Enerergy Convers Manage 63:87–94
17. García-Gracia M, Comech MP, Sallán J, Llombart A (2008) Modelling wind farms for grid disturbance studies. Renewable Energy 33:2109–2121
18. Ghennam T, Berkouk EM, Francois B (2009) Modeling and control of a Doubly Fed Induction Generator (DFIG) based wind conversion system. In: International conference on power engineering, energy and electrical drives, Lisbon, March 2009
19. Wei Q, Venayagamoorthy GK, Harley RG (2009) Real-Time implementation of a STATCOM on a wind farm equipped with doubly fed induction generators. IEEE Trans Ind Appl 45:98–107
20. Salman SK, Badrzadeh B (2004) New approach for modelling doubly-fed induction generator (DFIG) for grid-connection studies. European wind energy conference and exhibition, London, November 2004

21. SimPowerSystems (2010) – model and simulate electrical power systems. User's guide. Natick (MA): The Mathworks Inc
22. Voelker DH (2001) Statistics. John Wiley and Sons Inc, New York
23. Senjyu T, Sakamoto R, Urasaki N, Funabashi T, Fujita H, Sekine H (2006) Output power leveling of wind turbine generator for all operating regions by pitch angle control. IEEE Trans Energy Convers 21:467–475
24. Slootweg JG (2003) Wind power: modelling and impact on power system dynamics. Dissertation, Delft University of Technology
25. Engelhardt S, Erlich I, Feltes C, Kretschmann J, Shewarega F (2011) Reactive power capability of wind turbines based on doubly fed induction generators. IEEE Trans Energy Convers 26:364–372
26. Magnusson M, Smedman AS (1999) Air flow behind wind turbines. J Wind Eng Ind Aerodyn 80:169–189
27. Rudion K (2008) Aggregated modelling of wind farms. Dissertation, Otto-von-Guericke University
28. Perdana A (2008) Dynamic models of wind turbines. Dissertation, Chalmers University of Technology
29. Trilla L, Gomis-Bellmunt O, Junyent-Ferre A, Mata M, Sanchez Navarro J, Sudria-Andreu A (2011) Modeling and validation of DFIG 3-MW wind turbine using field test data of balanced and unbalanced voltage sags. IEEE Trans Sustain Energy 2:509–519